Long-range epidemic spreading in a random environment

Róbert Juhász,[1,*] István A. Kovács,[1,2,3,†] and Ferenc Iglói[1,2,‡]

[1]*Wigner Research Centre for Physics, Institute for Solid State Physics and Optics, P.O. Box 49, H-1525 Budapest, Hungary*
[2]*Institute of Theoretical Physics, Szeged University, H-6720 Szeged, Hungary*
[3]*Center for Complex Networks Research and Department of Physics, 111 Dana Research Center, Northeastern University,*
110 Forsyth Street, Boston, Massachusetts 02115, USA

Modeling long-range epidemic spreading in a random environment, we consider a quenched, disordered, d-dimensional contact process with infection rates decaying with distance as $1/r^{d+\sigma}$. We study the dynamical behavior of the model at and below the epidemic threshold by a variant of the strong-disorder renormalization-group method and by Monte Carlo simulations in one and two spatial dimensions. Starting from a single infected site, the average survival probability is found to decay as $P(t) \sim t^{-d/z}$ up to multiplicative logarithmic corrections. Below the epidemic threshold, a Griffiths phase emerges, where the dynamical exponent z varies continuously with the control parameter and tends to $z_c = d + \sigma$ as the threshold is approached. At the threshold, the spatial extension of the infected cluster (in surviving trials) is found to grow as $R(t) \sim t^{1/z_c}$ with a multiplicative logarithmic correction and the average number of infected sites in surviving trials is found to increase as $N_s(t) \sim (\ln t)^\chi$ with $\chi = 2$ in one dimension.

I. INTRODUCTION

The contact process (CP) [1,2] is a basic model in the fields of epidemic spreading and population dynamics. It is defined on a lattice, the sites of which are either active or inactive. The activity spreads to other inactive sites (which is interpreted as spreading of the infection in the case of epidemic modeling) or vanishes (which is interpreted as the spontaneous recovery of the individual at that site) stochastically with given rates. This model has attracted much interest because it undergoes a continuous phase transition from a fluctuating active phase to an inactive one if the relative magnitude of infection rates with respect to the recovery rate is varied. In its simplest form, activity spreads to neighboring lattice sites with uniform rates. The phase transition of this variant falls into the universality class of directed percolation (DP) and the critical exponents are known with a high precision [3–5], although their exact values are unknown.

The contact process was later generalized in different directions and studied with a focus on the phase transition. Here we highlight two factors that have a substantial effect on the critical behavior. In the long-range contact process (LRCP), infection is not restricted to neighboring sites but allowed to occur on any other site with a rate that decays as a power of the distance $\lambda(r) \sim r^{-(d+\sigma)}$, where d denotes the dimension [6]. The critical exponents of this model have been calculated to first order in an ϵ expansion by a field-theoretic renormalization-group method [7]. It turned out that, in analogy with the long-range Ising and $O(N)$ models [8–12], the critical exponents vary continuously with σ in the range $\sigma_{MF}(d) < \sigma < \sigma_{DP}(d)$, while for $\sigma > \sigma_{DP}(d)$ the model is in the DP universality class and for $\sigma < \sigma_{MF}(d)$ the critical behavior is described by a mean-field theory. The

upper critical dimension of the LRCP is $d_c = \min(4, 2\sigma)$ and the correlation length critical exponents in the mean-field region ($d > d_c$) are $\nu_{MF}^\perp = \max(1/2, 1/\sigma)$ and $\nu_{MF}^\parallel = 1$. In the intermediate region $\nu^\perp(\sigma)$ [$\nu^\parallel(\sigma)$] is a monotonically decreasing (increasing) function of σ. Numerical simulations in one dimension have confirmed the above scenario [13]. Motivated by the dynamics of a fluctuating interface growing on a one-dimensional substrate, a restricted variant of the LRCP has been studied as well [14,15]. In this model, activation of a site occurs only by the nearest active site. The main difference in critical behavior of this variant compared to that of the unrestricted one is the absence of a mean-field region. Long-range epidemic spreading has also been studied by other models, such as the susceptible-infected-recovered model [16,17]. For further studies in this field, we mention Refs. [18–20].

Another circumstance that changes the critical behavior of CP is quenched disorder. According to a strong-disorder renormalization-group (SDRG) study in one dimension [21], the critical behavior is, at least for strong enough initial disorder, described by a so-called infinite-disorder fixed point (IDFP) [22,23], where the relationship between time τ and length scale ξ is extremely anisotropic $\ln \tau \sim \xi^\psi$. As a consequence, the disorder-averaged dynamical quantities, such as the survival probability, decay as a power of $\ln t$ rather than as a power of t. Furthermore, in close analogy to the Griffiths phase of quantum magnets [24], the dynamics in the inactive phase is characterized by power laws, where the exponents vary continuously with the control parameter [25,26].

In this work we aim at studying the dynamics of the CP in the simultaneous presence of the above components, i.e., long-range interactions and quenched disorder. This type of problem emerges in different situations. Here we mention the case when an infectious disease is transmitted by insects, which make occasionally long flights, the length of which has a power-law distribution. Similarly, human infections can be transported through long-distance plane flights and plant disease epidemics spread through atmospheric dispersal,

―――――――
*juhasz.robert@wigner.mta.hu
†kovacs.istvan@wigner.mta.hu
‡igloi.ferenc@wigner.mta.hu

which have also power-law characteristics [27]. In all cases the infection and recovery rates are generally position-dependent random variables. We shall see that the interplay of disorder and long-range interactions results in a critical behavior, which is different from those observed in the presence of only one component. The long-range random transverse-field Ising chain, which is closely related to the present problem due to a formally similar SDRG treatment, has been recently studied with the conclusion that the critical behavior is controlled by a strong-disorder fixed point with a power-law scaling [28]. By inspecting the SDRG scheme of the CP in one dimension, we will show that, in spite of the differences in the SDRG rules, the same conclusions hold also for this model. In addition to this, we will present results of a numerical SDRG study in two dimensions, as well as results of Monte Carlo simulations in one and two dimensions.

The rest of the paper is organized as follows. The model is defined in Sec. II and a phenomenological argument about a limiting value of the dynamical exponent in the Griffiths phase is given in Sec. III. A SDRG scheme of the model is presented in Sec. IV. Our results for the one-dimensional model are presented in Sec. V and for the two-dimensional model in Sec. VI. Finally, the results are discussed in Sec. VII and the details of the SDRG calculations are deferred to the Appendix.

II. MODEL

Let us consider a d-dimensional cubic lattice, the sites of which can be either active or inactive, and consider a continuous-time Markov process with the following (independent) transitions. Site i, if it is active, becomes spontaneously inactive with a rate μ_i or it activates site j, provided the latter is inactive, with a rate λ_{ij}. The activation rates are parametrized as follows:

$$\lambda_{ij} = \Lambda_{ij} r_{ij}^{-(d+\sigma)}, \tag{1}$$

where r_{ij} is the Euclidean distance between sites i and j, and Λ_{ij} are $O(1)$ independent and identically distributed quenched random variables drawn from some distribution $\pi(\Lambda)$. The recovery rates μ_i are also independent and identically distributed quenched random variables drawn from a distribution $\kappa(\mu)$. For the sake of brevity, we introduce the decay exponent α of the infection rates as $\alpha \equiv d + \sigma$. We will restrict ourselves to the regime $\alpha > d$, where the total rate of activation events from a given site $\lambda_i = \sum_{j \neq i} \lambda_{ij}$ remains finite.

This system exhibits two different phases. For a low enough tendency for recovery, such that $\overline{\ln \mu} - \overline{\ln \Lambda} = \theta < \theta_c$, the fraction of active sites in the stationary state is $\rho > 0$, which represents the active phase. (Here and in the following the overbar denotes an average over quenched disorder.) In contrast, for a high enough tendency for recovery $\theta > \theta_c$, we have $\rho = 0$ in the stationary state. In between, at $\theta = \theta_c$, there is a nonequilibrium phase transition in the system, the properties of which are the subject of this work.

Although we will consider a finite strength of disorder, as a first step, it is worth investigating the stability of the fixed point of the clean system (with long-range infections) against weak disorder. Generalizing the heuristic criterion by Harris [25,29] for long-range interactions, weak disorder is predicted to be relevant if

$$d\nu^\perp < 2, \tag{2}$$

where $\nu^\perp$ is the correlation-length exponent of the nonrandom system. According to the known results for $\nu^\perp$, discussed in the Introduction, weak disorder is generally relevant, except in the mean-field region, where it is irrelevant.

III. PHENOMENOLOGICAL THEORY IN THE GRIFFITHS PHASE

In the short-range random CP, where activation occurs only on neighboring sites, the average density, i.e., the fraction of active sites $\rho(t)$, decays as an inverse power of time starting from a fully active initial state, in a regime $\theta_c < \theta < \theta_G$ of the inactive phase, called the Griffiths phase [25]. This type of semicritical behavior (short-range spatial, but long-range dynamical correlations) can be explained by a phenomenological theory (for a review see, e.g., Ref. [26]). According to this, although the entire system is subcritical on average and tends toward the absorbing (inactive) state for long times, it still contains clusters of sites, the so-called rare regions, where the majority of internal activation rates are greater than the average, so the local control parameter θ_l is below the bulk critical point; thus these regions are locally supercritical. A probability of occurrence of rare regions is exponentially small but their lifetime is exponentially large in their size, so the distribution of their lifetimes has an algebraic tail

$$P_>(\tau) \sim \tau^{-d/z}, \tag{3}$$

characterized by a nonuniversal dynamical exponent z, which depends on the distance from the critical point $z = z(\theta)$ and diverges as the critical point is approached. If the initial state of the model is the fully active one, then after a long time, the activity will survive in clusters having a lifetime greater than t. Let us denote the characteristic distance between nearest active clusters at time t by $\ell(t)$. At time t, the fraction of active clusters is on the one hand on the order of $1/\ell^d(t)$, while on the other hand it is proportional to $P_>(t)$. Using Eq. (3), we have thus

$$\ell(t) \sim t^{1/z}, \tag{4}$$

the usual relation between length and time scales. The typical (effective) activation rate between nearest active clusters at time t is exponentially small in $\ell(t)$: $\lambda_{\text{eff}}[\ell(t)] \sim \exp[-c\ell(t)]$, so the active clusters, which have a typical lifetime $O(t)$ or, equivalently, $O[\ell^z(t)]$, do not interact with each other for long times and each of them arrives at the inactive state at a time determined by its own lifetime, which has been tacitly assumed. Using that the mass of clusters (i.e., number of sites contained in it) that are active at time t is at most $m(t) = O(\ln t)$, one obtains for the time dependence of the average density

$$\rho(t) \sim m(t) P_>(t) \sim t^{-d/z} \tag{5}$$

up to logarithmic corrections.

Let us now see how the above picture is modified in the case of long-range interactions. In the following reasoning, we assume that the relevant time scale in the problem is governed

by the supercritical rare regions as in the short-range case and thus the relations in Eqs. (3) and (4) are valid with an appropriate value of the dynamical exponent $z(\theta)$. However, due to the long-range interactions, the typical activation rates between neighboring active clusters are different and these are estimated to be $\lambda_{\mathrm{eff}}[\ell(t)] \sim \ell^{-\alpha}(t)m^2(t)$. Here the typical mass of an active cluster $m(t)$ is expected to be a slower-than-algebraic (logarithmic) function of time. For a fixed pair of neighboring active clusters, the characteristic time between two subsequent activation events thus scales as $\tau_a \sim 1/\lambda_{\mathrm{eff}}[\ell(t)] \sim \ell^{\alpha}(t)m^{-2}(t)$. These clusters can be regarded as independent if τ_a is much greater than the typical lifetimes of the clusters $\tau_l \sim \ell^z(t)$. Independence is realized asymptotically if $\tau_l(\ell)/\tau_a(\ell) \to 0$ as $\ell \to \infty$ ($t \to \infty$), yielding

$$z < \alpha, \tag{6}$$

which is a necessary condition for the self-consistency of the above phenomenological picture. We have thus obtained that, for a fixed α, the dynamical exponent in the Griffiths phase cannot increase unboundedly as the critical point is approached, but this phase must terminate at a point where z reaches the boundary value α. At this point, the above picture breaks down since the clusters no longer die out independently and the infection rates and recovery rates become comparable with each other. This suggests that this point coincides with the phase transition point separating the Griffiths phase from the active phase so that

$$\lim_{\Theta \to \Theta_c+} z(\Theta) = \alpha. \tag{7}$$

IV. STRONG-DISORDER RENORMALIZATION-GROUP TREATMENT

In the strong-disorder renormalization-group approach to the contact process [21,23], the transition with the highest rate is iteratively eliminated and the effective rates of the reduced system are calculated perturbatively. Thereby the actually highest rate Ω of the renormalized system is gradually reduced. The procedure consists of two kinds of reduction steps and here we recapitulate the results in [21]. If the largest rate is an activation rate $\Omega = \lambda_{ij}$, sites i and j form a cluster, which has an effective deactivation rate

$$\tilde{\mu}_{ij} \simeq \frac{2\mu_i\mu_j}{\Omega} \tag{8}$$

if $\mu_i, \mu_j \ll \lambda_{ij}$. If the largest rate is a deactivation rate $\Omega = \mu_i$, cluster i is deleted and clusters that were neighboring i become directly connected through an effective activation rate

$$\tilde{\lambda}_{jk} \simeq \frac{\lambda_{ji}\lambda_{ik}}{\Omega} \tag{9}$$

if $\lambda_{ji}\lambda_{ik} \ll \mu_i$. Apart from one-dimensional systems, for which the above procedure was originally developed [22,30], double connections between clusters may appear after performing the above reduction steps. This is treated in practice in two different ways. The rates of the two parallel transitions are either added, which is termed a sum rule, or the larger one of them is kept, in which case we speak about a maximum rule. In the case of an IDFP, which governs the critical behavior of the short-range CP, the SDRG with both rules

becomes asymptotically exact and is conjectured to provide correct critical exponents [23]. The random transverse-field Ising model (RTIM) has an SDRG scheme identical to that of the CP, apart from the absence of the factor 2 in Eq. (8) [22]. This difference is irrelevant in the critical properties of the two models for short-range interactions and we expect the same conclusion for the long-range models too.

For the RTIM, the SDRG procedure with the maximum rule can be implemented in a very efficient numerical algorithm [31], which provides accurate results for the short-range model in higher dimensions too. This numerical procedure has been used for the one-dimensional long-range RTIM and the observed renormalization steps are summarized in an approximate primary model, which has been analytically solved [28,32]. Here we generalize these steps for the one-dimensional LRCP and the results are summarized in Sec. V. For the two-dimensional model, results of the numerical analysis with the RTIM maximum rule are presented in Sec. VI.

V. RESULTS FOR THE ONE-DIMENSIONAL MODEL

A. The SDRG analysis

A simplified SDRG scheme of the one-dimensional random LRCP, which we call a primary scheme, is presented in the Appendix together with its analytical solution. In this approach, the renormalized system has a one-dimensional structure with effective interactions only between neighboring (nondecimated) clusters. Long-range interactions between remote clusters are taken into account only at a later stadium of the renormalization procedure, when these clusters become nearest neighbors. A further simplification in the primary scheme is that the effective interactions between clusters are approximated by the long-range interaction between the closest constituent sites of clusters. In this respect, this treatment is closer to a disordered variant of the restricted LRCP mentioned in the Introduction [14,15]. Unfortunately, an extension of the primary scheme, which takes into account all pair interactions between neighboring clusters and is more appropriate to describe the unrestricted model, cannot be solved *ab initio*; nevertheless, its scaling properties can be inferred from those of the primary scheme by heuristic reasoning.

Before presenting the results obtained by the SDRG method, a caveat is in order concerning its reliability. We will see that the critical behavior of the model is described by a strong-disorder fixed point, where the disorder remains finite, rather than by an IDFP. In this case, the asymptotic exactness of the method is not guaranteed, therefore the outcomes of the method must be confronted with results of Monte Carlo simulations of the original model. Nevertheless, for another example of a model with a strong-disorder fixed point, namely, the two-dimensional random Heisenberg model, the predictions of the method have been proven qualitatively correct [33].

The main results of the analysis of the primary scheme are summarized in Eqs. (10) and (11) below. A relationship between the rate scale Ω and the length scale ℓ, which is the inverse of the concentration of nondecimated clusters, is

provided by the method in the form

$$\ell \simeq \ell_0 \left(\frac{\Omega_0}{\Omega}\right)^{1/\alpha} \left[\frac{1}{\alpha} \ln \frac{\Omega_0}{\Omega}\right]^2, \tag{10}$$

which follows from Eq. (A13), where Ω_0 is the initial rate scale and ℓ_0 is a nonuniversal constant depending on the distribution of rates. Another important quantity is the survival probability $Q(\Omega)$ of a given site during the SDRG procedure, which is found to decay with Ω as given in Eq. (A16) or in terms of the length scale

$$Q(\ell) \sim \frac{\ell_0}{\ell} \left[\ln \frac{\ell}{\ell_0}\right]^2. \tag{11}$$

The results in Eqs. (10) and (11) are obtained for the primary model, in which the SDRG scheme is based on the maximum rule. These results can be somewhat improved by using a scheme that works partially by the sum rule; see [28] for the RTIM. It takes into account, namely, the interactions between all pairs of sites of neighboring clusters and, as it has been argued and confirmed numerically, this improved scheme is roughly mapped to the primary scheme if it is formulated in terms of reduced variables $\lambda/m^2(\ell)$ and $\mu/m^2(\ell)$, where $m(\ell) = Q(\ell)\ell$ is the average mass of nondecimated clusters at the length scale ℓ. This means that improved scaling relations are obtained from those of the primary scheme by replacing Ω with $\Omega/[Q(\ell)\ell]^2$. This leaves the scaling of $Q(\ell)$ in Eq. (11) in leading order unchanged, but affects the power of the logarithmic correction in the dynamical relation in Eq. (10), resulting in

$$\ell \sim \left(\frac{\Omega_0}{\Omega}\right)^{1/\alpha} \left(\ln \frac{\Omega_0}{\Omega}\right)^{2+4/\alpha}. \tag{12}$$

We will use this relation in the following.

B. Scaling at criticality

The scaling properties of different observables at the critical point can be obtained from Eqs. (11) and (12) as follows. Starting the process from a fully active state, Eq. (12) provides a relationship for the typical time $t = \Omega^{-1}$ needed for a segment of size ℓ in an infinite system or, for a finite system of size ℓ, to settle in a quasistationary state, in which only the largest cluster identified by the SDRG method in the given segment is active and the other sites are typically inactive. The average fraction of active sites $\rho(L)$ in the quasistationary state of finite systems of size L scales as

$$\rho(L) \sim Q(L) \sim L^{-1}(\ln L)^2, \tag{13}$$

where we have used Eq. (11). However, in the numerical simulations to be presented in the next section, we have studied the time dependence of various quantities as the process approaches the stationary state rather than considering stationary ones. To be concrete, starting the process from a single active site, we are interested in the time-dependent average survival probability $P(t)$, which is the probability that the process has not yet been trapped in the absorbing (inactive) state at time t. Other quantities commonly studied with the above setup is the average number $N(t)$ of active sites at time t and the spread characterizing the spatial extension of the

growing cluster of active sites, defined as

$$R(t) = \exp\left\{\left\langle \overline{\frac{\sum_{i \neq 0} n_i(t) \ln r_i}{\sum_i n_i(t)}}\right\rangle_s\right\}. \tag{14}$$

Here $n_i(t)$ is 1 (0) if site i at time t is active (inactive), r_i denotes the Euclidean distance from the initially active site 0, and $\langle\cdot\rangle_s$ denotes the expectation value under the condition that the process is active at time t in a fixed random environment (i.e., set of transition rates). Note that the common definition of the spread for the short-range CP through the second moment of the distance from the origin would be divergent in the LRCP for any finite t, hence the average of the logarithmic distance, which is finite, is considered here instead [13]. Due to the self-dual property of the CP [2,34], the average survival probability $P(t)$ is equal to the average density $\rho(t)$ in the case when the process had been started from a fully active state. Expressing the length L in Eq. (13) with time $t \sim 1/\Omega$ using Eq. (12), we obtain for the asymptotic time dependence of the average survival probability at the critical point

$$P(t) = \rho(t) \sim [t(\ln t)^4]^{-1/\alpha}. \tag{15}$$

We can see that the critical decay exponent $1/\alpha$ coincides with the limiting value of the decay exponent at the upper boundary of the Griffiths phase found by the phenomenological theory in the previous section [see Eq. (7)]. The average number of active sites scales with the length ℓ as $N(\ell) \sim \frac{(\ln \ell)^2}{\ell}(\ln \ell)^2$, where the first factor is the probability that the starting site was part of the largest cluster in a segment of length ℓ and the second one is the mass of the largest cluster. Using Eq. (12), we obtain

$$N(t) \sim [t(\ln t)^{4-2\alpha}]^{-1/\alpha} \tag{16}$$

for large t. Thus, the average number $N_s(t)$ of active sites in surviving samples scales with time as

$$N_s(t) = \frac{N(t)}{P(t)} \sim (\ln t)^2 \tag{17}$$

irrespective of α. As it has been argued in Ref. [28], the length of the longest bond in the largest cluster of a segment of length ℓ is $O(\ell/(\ln \ell)^4)$. Assuming that the length of the cluster, which roughly determines the spread, is in this order of magnitude and using Eq. (12), the spread is expected to scale with time asymptotically as

$$R(t) \sim [t(\ln t)^{4-2\alpha}]^{1/\alpha}. \tag{18}$$

C. Numerical simulations

We have performed discrete-time Monte Carlo simulations of the disordered LRCP on rings of $L = 10^9$ sites. The disorder was implemented by a random dilution, i.e., the fraction c of sites was removed. The simulation consisted of the following moves. An active site is chosen randomly and with a probability $1/(1 + \lambda)$ it is made inactive or with a probability $\lambda/(1 + \lambda)$ a random variable r from an algebraic distribution with the probability density $f(r) = (\alpha - 1)r^{-\alpha}$ in the range $(1,\infty)$ is generated. Then one of the two sites whose distance from the active site is the integer part of $r \mod L$ is chosen with equal probability as a target site. If the target site is an existing
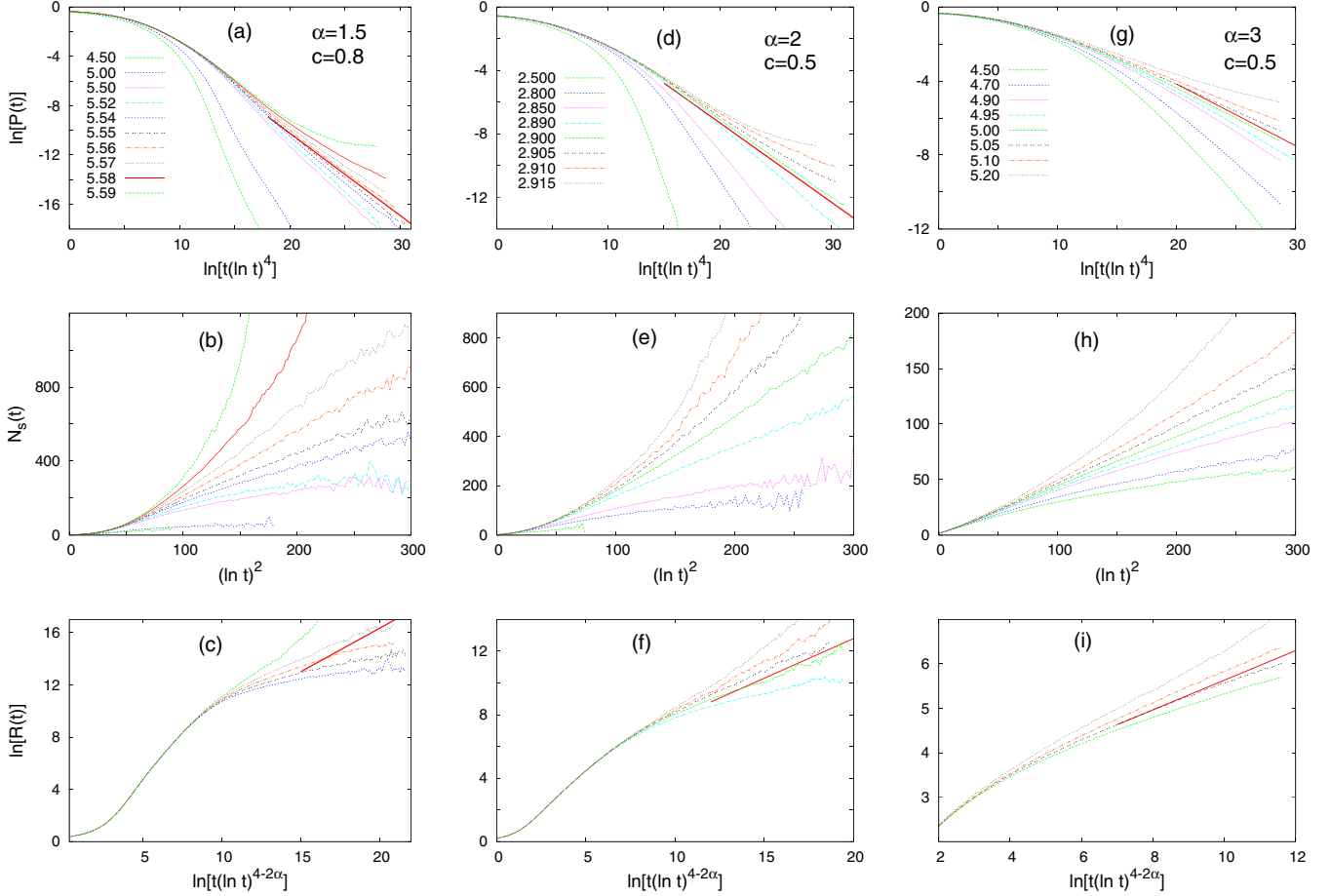
FIG. 1. (Color online) (a), (d), and (g) Logarithm of the average survival probability $P(t)$ plotted against $\ln[t(\ln t)^4]$. The data were obtained by numerical simulations of the one-dimensional model for different values of the control parameter λ. The solid line with a slope $-1/\alpha$ indicates the asymptotic behavior predicted by the SDRG approach of the model at the critical point. (b), (e), and (h) Average number $N_s(t)$ of active sites conditioned on survival plotted against $(\ln t)^2$. (c), (f), and (i) Logarithm of the spread $R(t)$ defined in Eq. (14) plotted against $\ln[t/(\ln t)^{2\alpha-4}]$. The solid line with a slope $1/\alpha$ indicates the asymptotic behavior predicted by the SDRG approach of the model at the critical point.

and inactive site, it will be activated. One Monte Carlo step (of unit time) consists of $n(t)$ such moves, where $n(t)$ is the number of active sites at the beginning of the Monte Carlo step. Starting the process from a single active site, we have followed the simulation up to $t = 2^{27}$ Monte Carlo steps. Repeating the simulation for 10–1000 randomly diluted lattices and for 10^5 starting positions per sample, we have calculated the average survival probability $P(t)$, the average number of active sites $N(t)$, and the spread $R(t)$ as a function of time for different values of the decay exponent α, the dilution parameter c, and the control parameter λ.

According to the Harris criterion in Eq. (2), weak disorder is predicted to be relevant in one dimension if $\alpha > 3/2$. Numerical results for $\alpha = 2, 3$ with $c = 0.5$ are shown in Figs. 1(d)–1(i). In these cases, a Griffiths phase can be identified where the survival probability decays algebraically with time (with possible logarithmic corrections). The decay exponent varies continuously with λ and at a critical value λ_c the time dependence is compatible with the form given in Eq. (15). The critical point is estimated to be at $\lambda_c = 2.90(1)$ for $\alpha = 2$ and $\lambda_c = 5.00(5)$ for $\alpha = 3$. At this point, the time

dependence of the average number of active sites in surviving trials is compatible with the square-logarithmic law given in Eq. (17). The predicted behavior of the spread given in Eq. (18) fits satisfactorily to the data for $\alpha = 2$ but for $\alpha = 3$ a slight discrepancy can be observed.

Simulations with the marginal decay exponent $\alpha = 3/2$ and for a dilution $c = 0.8$ have shown a behavior similar to that found for $\alpha > 3/2$, as can be seen in Figs. 1(a)–1(c). For a weaker dilution $c = 0.5$, however, the critical behavior rather seems to be compatible with that of the clean LRCP, as shown in Figs. 2(a)–2(c). Here, at the border of the mean-field regime, the survival probability decays as $P(t) \sim t^{-1}(\ln t)^{3/7}$, the exponent η, characterizing the growth of the number of active sites $N(t) \sim t^\eta$, is zero, and the spread increases as $R(t) \sim t^{1/z}$ with $z = \sigma$ [7]. Note that, due to the rapid increase of the spread [$R(t) \sim t^2$ for $\alpha = 3/2$], the times for which finite-size effects are negligible are much shorter than in the case of the strong-disorder scenario. From measurements in this limited range of time, it cannot be decided whether this is the true asymptotic behavior or a crossover to the strong-disorder fixed point occurs at larger time scales.
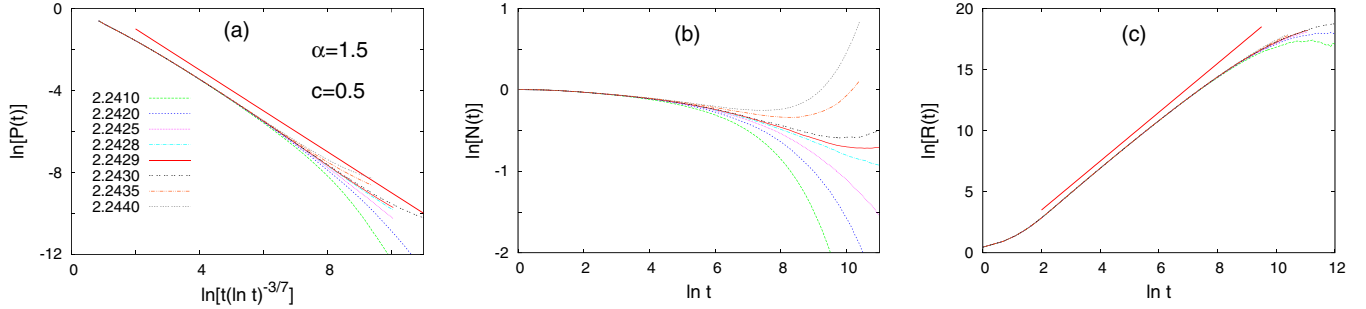
FIG. 2. (Color online) (a) Logarithm of the average survival probability $P(t)$ plotted against $\ln[t(\ln t)^{-3/7}]$. The solid line has a slope -1. The data were obtained by numerical simulations of the one-dimensional model with $\alpha = 3/2$ and $c = 0.5$ for different values of the control parameter λ. (b) Logarithm of the average number of active sites $N(t)$ plotted against $\ln t$. (c) Logarithm of the spread $R(t)$ plotted against $\ln t$. The solid line has a slope $1/\sigma = 2$.

VI. RESULTS FOR THE TWO-DIMENSIONAL MODEL

A. Relation to the one-dimensional model

Before presenting Monte Carlo results of the two-dimensional model, let us sketch a simple argument for the scaling behavior of the quantities of interest in higher dimensions. Let us start with the model with a decay exponent α, on a d-dimensional hypercubic lattice of (finite but large) size L, which is assumed to be an integer power of 2. Let us divide the hypercube into 2^d smaller hypercubes and arrange them in chain (in arbitrary order). Then we iterate this step for the smaller hypercubes until we arrive at a linear chain of length L^d. After this procedure, almost all distances ℓ between spins in the original hypercube will be $O(\ell^d)$. So we roughly obtain in this way a one-dimensional model with a reduced decay exponent α/d. As a first guess for the scaling behavior in d dimensions, we take the formulas obtained in one dimension and replace the quantities having a length dimension ℓ with ℓ^d and α with α/d in them [35]. This results in

$$P(t) \sim [t(\ln t)^4]^{-d/\alpha}, \tag{19}$$

$$R(t) \sim [t(\ln t)^{4-2\alpha/d}]^{1/\alpha}, \tag{20}$$

which is expected to be correct for the powers of algebraic factors but not those of logarithmic corrections. Indeed, the relations in Eqs. (19) and (20) are in agreement with Eqs. (5) and (4), respectively, at least up to logarithmic corrections. The scaling form of N_s in Eq. (17), which is purely logarithmic, is expected to be so for $d > 1$, as well:

$$N_s(t) \sim (\ln t)^\chi, \tag{21}$$

with a possibly different power $\chi \geqslant 2$.

B. The SDRG analysis

In two dimensions, the SDRG method can only be implemented numerically; here we refer to the SDRG studies of the short-range RTIM in two and higher dimensions. In order to have a more efficient numerical algorithm, we have used the maximum rule and in the renormalization rule in Eq. (8) we omitted the factor 2. In the one-dimensional case, these simplifications are found not to modify the critical properties of the system and the same type of irrelevance is expected to hold in two dimensions too. For this problem we have used

an algorithm that has been developed by us for the RTIM and used recently to analyze the critical properties of the long-range model in one dimension. In the two-dimensional case we have renormalized finite samples of linear size up to $L = 64$. The number of samples were typically $160\,000$ (at least 4000 for the largest size). The parameters of the model were chosen uniformly from the intervals $\Lambda_{ij} \in (0,1]$ and $\mu_i \in (0,\mu]$, with a control parameter $\theta = \ln(\mu)$. We have fixed the decay exponent to $\alpha = 3$, in which case the critical point is found at $\theta_c = 2.42(5)$ from the analysis of the distributions of the sample-dependent critical points. (For details of the method we refer the reader to Ref. [28].) At the critical point, we have calculated two quantities: the average mass of the last remaining cluster $m(L) = L\,Q(L)$ [see Eq. (13)] and the characteristic time scale $\tau(L)$ defined as $\tau = 1/\tilde{\mu}$, where $\tilde{\mu}$ is the last decimated parameter in a finite sample.

The numerical results indicate that $m(L)$ has a slower-than-algebraic dependence, which can be written in analogy with the one-dimensional result in Eq. (13) as $m(L) \sim [\ln(L/L_0)]^\chi$. Precise determination of χ from the existing numerical results is difficult since it is sensitive to the value of the reference length L_0. The data in Fig. 3 are compatible with $\chi = 2$ with $L_0 = 3$, but a similar fit is obtained with $\chi = 3$ if we choose $L_0 = 0.5$ instead.
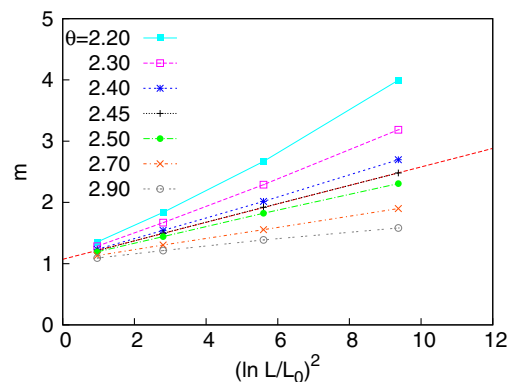

FIG. 3. (Color online) Average mass of the last decimated cluster plotted against $(\ln L/L_0)^2$ with $L_0 = 3$. The data were obtained by numerical renormalization of the two-dimensional model with decay exponent $\alpha = 3$ for different values of the control parameter Θ.
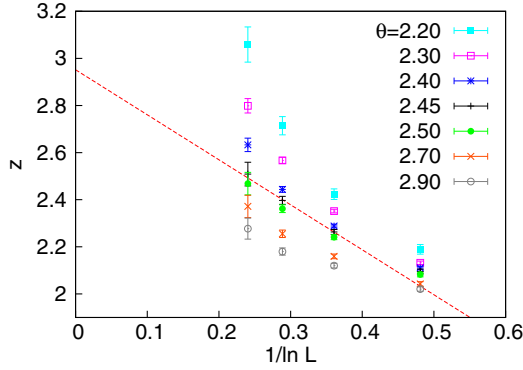
FIG. 4. (Color online) Effective dynamical exponents obtained by two-point fits using Eq. (22) as a function of the system size L. The straight line is a fit to the data obtained for $\Theta = 2.45$.

Calculating the average logarithmic time scale $\overline{\ln \tilde{\tau}}$, estimates of an effective size-dependent dynamical exponent $z(L)$ have been obtained from two-point fits of the relation

$$\overline{\ln \tilde{\tau}} = z \ln L + \text{const}. \tag{22}$$

The extrapolation of $z(L)$ to infinite system size, as shown in Fig. 4, is compatible with the expectation $z_c = \alpha$.

C. Numerical simulations

We have performed Monte Carlo simulations of the two-dimensional model on diluted lattices of linear size $L = 40\,000$. In the case of infection events, the target sites have been chosen as described in Ref. [16]. For each set of parameters (α, c, λ), seed simulations have been carried out in 100–1000 randomly diluted lattices, for 160 000 different starting positions in each sample, and averages of dynamical quantities have been calculated.

In two dimensions, the Harris criterion in Eq. (2) predicts weak disorder to be relevant if $\alpha > 3$. In this domain, we have detected a Griffiths phase and obtained that the critical behavior is satisfactorily compatible with the predictions of the SDRG method extended to $d > 1$ [see Eqs. (19)–(21)] apart from poor agreement in the case of the time dependence of the spread. The exponent χ describing the increase of the average number of active sites in surviving trials in Eq. (21) is found to be compatible with the value $\chi = 2$ characterizing the one-dimensional model. As an illustration, we show results obtained for $\alpha = 3.5$ and $c = 0.8$ in Figs. 5(d)–5(f). The
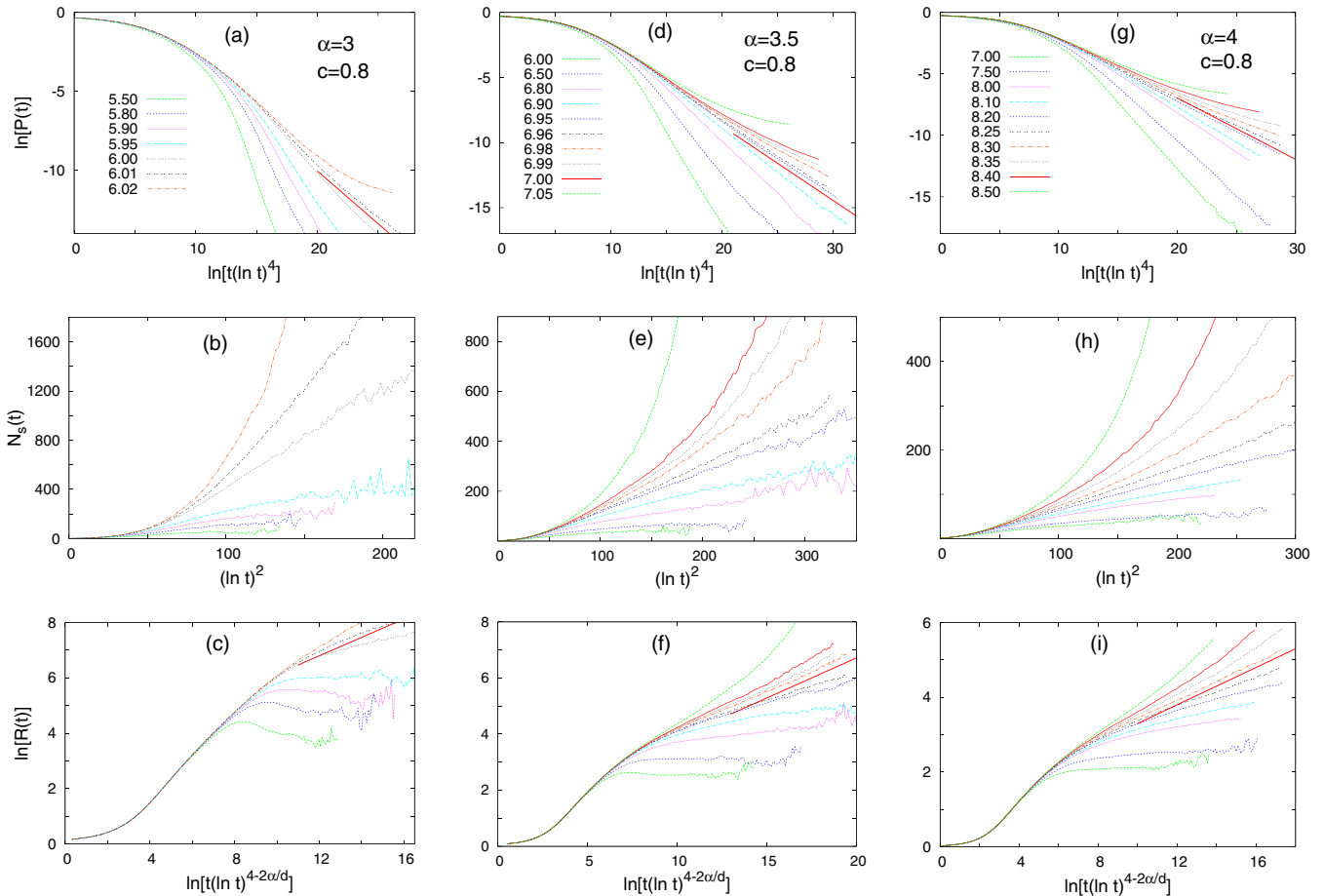

FIG. 5. (Color online) (a), (d), and (g) Logarithm of the average survival probability $P(t)$ plotted against $\ln[t(\ln t)^4]$. The solid line has a slope $-d/\alpha$. The data were obtained by numerical simulations of the two-dimensional model for different values of the control parameter λ. (b), (e), and (h) Average number $N_s(t)$ of active sites conditioned on survival plotted against $(\ln t)^2$. (c), (f), and (i) Logarithm of the spread $R(t)$ defined in Eq. (14) plotted against $\ln[t/(\ln t)^{2\alpha/d-4}]$. The solid line has a slope $1/\alpha$.
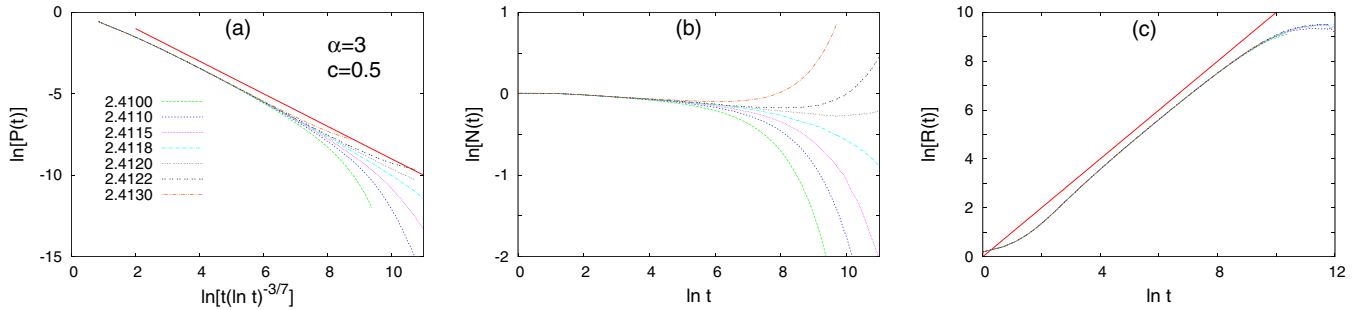
FIG. 6. (Color online) (a) Logarithm of the average survival probability $P(t)$ plotted against $\ln[t(\ln t)^{-3/7}]$. The solid line has a slope -1. The data were obtained by numerical simulations of the two-dimensional model with $\alpha = 3$ and $c = 0.5$ for different values of the control parameter λ. (b) Logarithm of the average number of active sites $N(t)$ plotted against $\ln t$. (c) Logarithm of the spread $R(t)$ plotted against $\ln t$. The solid line has a slope $1/\sigma = 1$.

critical point is estimated to be at $\lambda_c = 6.95(3)$. Similar conclusions have been obtained for $\alpha = 4$ and $c = 0.8$ [see Figs. 5(g)–5(i)] and for $\alpha = 3.5$ and $c = 0.5$ (not shown).

For the decay exponent $\alpha = 3$, at which, according to the Harris criterion, weak disorder is marginal, the strong-disorder fixed point still seems to describe the critical behavior of the model for a strong enough dilution, as shown for $c = 0.8$ in Figs. 5(a)–5(c). The critical point is estimated to be at $\lambda_c = 6.01(1)$. For a weaker dilution, however, as it is illustrated by the data in Figs. 6(a)–6(c) obtained for $c = 0.5$, no Griffiths effects can be observed and the critical behavior seems to agree with that of the clean LRCP, which is described by the mean-field theory, rather than with the strong-disorder scenario. These numerical results thus suggest that, fixing the decay exponent to its marginal value $\alpha = 3$, the disorder changes from irrelevant to relevant as its strength is increased. Note that a similar scenario has been found numerically for the disordered short-range CP in Ref. [21,36]; see, however, the conflicting results in Refs. [37,38]. We stress again that the time interval in which the model is free from finite-size effects [see Fig. 6(c)] is rather short and in this regime no definite conclusions can be drawn concerning the asymptotic behavior from the numerical data.

We have simulated the model with $\alpha = 2.5$ and $c = 0.8$ as well, which belong to the domain where weak disorder is predicted to be irrelevant by the Harris criterion. Here mean-field critical behavior is found (not shown) and within the very short time scale, where the system is free from finite-size effects, no indications of the existence of a Griffiths phase have been seen. It is interesting to compare these observations with the behavior of the disordered short-range contact process above its upper critical dimension $d_c = 4$, where weak disorder is irrelevant, just as in our case. According to a recent conjecture, which is supported by simulation results for $d = 5$ [39], the critical behavior is of mean-field type but a Griffiths phase still shows up, where the dynamical exponent varies with the control parameter and saturates to the mean-field value. The numerical results obtained for our model fit only partially to this scenario, as Griffiths effects could not be observed in our case.

VII. DISCUSSION

In this paper we have studied a long-range contact process in a random environment. This model is realized in different situations, when the agents transmitting the disease can be insects, human beings, or spores. Depending on the relative strengths of the infection and the recovery rates, this model exhibits an active (endemic) phase with a finite fraction of infected sites in the steady state and an inactive one, where all sites are healthy. The properties of the nonequilibrium phase transition in the system are studied by different methods in one and two spatial dimensions.

Analytical results are obtained in one dimension by a variant of the SDRG method, which is called the primary scheme. The critical point is found to be controlled by a so-called strong-disorder fixed point, in which the dynamical exponent is finite and given by $z_c = \alpha$ in any dimension. The average number of active sites in surviving samples is found to increase as $N_s(t) \sim (\ln t)^\chi$, with $\chi = 2$ in $d = 1$, thus the set of active sites has a formally zero fractal dimension. In the nearby inactive Griffiths phase, the decay of the average density and the growth of the average spatial extent of the set of active sites still follow power laws, however the dynamical exponent is $z < \alpha$ and continuously depends on the distance from the transition point. The theoretical predictions obtained by the approximative SDRG method and phenomenological reasoning have been confronted with results of large-scale Monte Carlo simulations. We have found satisfactory agreement in the non-mean-field regime of the clean model $\alpha > \frac{3}{2}d$, where the Harris criterion predicts relevance of weak disorder. At the boundary of this regime $\alpha = \frac{3}{2}d$, the numerical data are compatible with the strong-disorder scenario only for a strong enough initial disorder; otherwise, as well as for $\alpha < \frac{3}{2}d$, they rather seem to follow the mean-field theory of the clean model. We emphasize, however, that, for judging the long-time asymptotic behavior in the mean-field regime, the present numerical results are not decisive and a crossover to a strong-disorder fixed point at large scales, even for a weak disorder, cannot be excluded. We mention that, even in the simplest case, i.e., in the one-dimensional short-range CP, although large-scale simulations suggest a positive answer [37], it is an unresolved question whether the IDFP is attractive for any weak disorder [40]. The situation observed in our model for $\alpha \leqslant \frac{3}{2}d$ is similar to that of the short-range CP at and above the upper critical dimension $d_c = 4$, where, although the SDRG approach predicts an IDFP in any dimensions for a strong enough disorder [31], numerical simulations indicate a mean-field critical behavior [39]. How

the nature of the phase transition changes with the strength of the disorder in this case is a puzzling question.

It is worth comparing the behavior of our model to that of the contact process on static (i.e., time-independent) random networks embedded in a d-dimensional space and having long-range links between remote sites with an algebraically decaying connection probability $p(l_{ij}) \sim l_{ij}^{-s}$ [41,42]. This model can be regarded as a quenched variant of the LRCP, where the randomly drawn long-range links induce quenched topological disorder. According to a numerical SDRG analysis of the one-dimensional model [42], for $s \geqslant 2$, the critical behavior is controlled by an IDFP, which is identical to that of the short-range disordered CP for $s > 2$. For $s < 2$, Monte Carlo simulations of the model show that the critical dynamics is described by power laws and no signs of Griffiths effects can be observed. An apparent difference between the two models is that the quenched model displays short-range behavior for a sufficiently large decay exponent ($s > 2$), while this is not the case for the disordered LRCP.

The results presented in this work are similar to that obtained very recently for the long-range RTIM. Indeed, the SDRG decimation steps differ only at one point in the two problems, which has been shown to be irrelevant in one dimension (see the Appendix). The same conclusion is expected to hold in higher dimensions too, which is demonstrated in Sec. VI for the two-dimensional case. For the RTIM, analysis of the primary model on the paramagnetic side of the critical point, which corresponds to the inactive phase of our model, leads to a divergence of the correlation length ξ of the form

$$\xi \sim \exp(A/|\theta - \theta_c|), \tag{23}$$

which resembles the singularity present in the Kosterlitz-Thouless transition. We expect that Eq. (23) holds for the LRCP as well. However, a numerical verification of this conjecture is very difficult.

APPENDIX: THE PRIMARY SDRG SCHEME IN ONE DIMENSION

Let us restrict ourselves to one dimension and assume that $\Lambda_{ij} = 1$ in Eq. (1), i.e., the activation rates are nonrandom, but the deactivation rates are still random. This model is, according to numerical investigations, in the same universality class as the one with random activation rates, but it is simpler to treat analytically. Analyzing the SDRG procedure close to the fixed point in the inactive phase and in the critical point, we have

a few observations that can be used to simplify the SDRG scheme. These observations are analogous to those found for the one-dimensional RTIM [28]. First, almost always, cluster eliminations occur; second, after decimating a cluster, the maximum rule leads almost always to $\tilde{\lambda}_{jk} = \lambda_{jk}$; third, the extensions of (nondecimated) clusters are typically much smaller than the distances between them. These lead to a simplified scheme of effectively one-dimensional structure, in which only the activation rates between neighboring clusters are renormalized. Introducing the reduced parameters $\zeta = (\frac{\Omega}{\lambda})^{1/\alpha} - 1$ and $\beta = \frac{1}{\alpha} \ln \frac{\Omega}{\mu}$, in analogy with the RTIM, the renormalization rules assume the additive forms

$$\tilde{\zeta} = \zeta_{i-1,i} + \zeta_{i,i+1} + 1 \tag{A1}$$

if a cluster is decimated and

$$\tilde{\beta} = \beta_i + \beta_{i+1} - B \tag{A2}$$

if two clusters are unified. The difference compared to the SDRG rules of the long-range RTIM is the appearance of constant $B = \frac{1}{\alpha} \ln 2$. We mention that the SDRG scheme with $B = 0$ first arose in the context of a disordered quantum rotor model [43]. As the logarithmic rate scale

$$\Gamma \equiv \frac{1}{\alpha} \ln \frac{\Omega_0}{\Omega}, \tag{A3}$$

with Ω_0 being the initial value of Ω, increases during the procedure, the distributions $g_\Gamma(\beta)$ and $f_\Gamma(\zeta)$ evolve according to the equations

$$\frac{\partial g_\Gamma(\beta)}{\partial \Gamma} = \frac{\partial g_\Gamma(\beta)}{\partial \beta} + f_0(\Gamma)$$
$$\times \int d\beta_1 \int d\beta_2 g_\Gamma(\beta_1) g_\Gamma(\beta_2) \delta(\beta - \beta_1 - \beta_2 + B)$$
$$+ g_\Gamma(\beta)[g_0(\Gamma) - f_0(\Gamma)], \tag{A4}$$

$$\frac{\partial f_\Gamma(\zeta)}{\partial \Gamma} = (\zeta + 1) \frac{\partial f_\Gamma(\zeta)}{\partial \zeta} + g_0(\Gamma)$$
$$\times \int d\zeta_1 \int d\zeta_2 f_\Gamma(\zeta_1) f_\Gamma(\zeta_2) \delta(\zeta - \zeta_1 - \zeta_2 - 1)$$
$$+ f_\Gamma(\zeta)[f_0(\Gamma) + 1 - g_0(\Gamma)], \tag{A5}$$

where $g_0(\Gamma) \equiv g_\Gamma(0)$ and $f_0(\Gamma) \equiv f_\Gamma(0)$.

At the critical point and below, the variables ζ will grow without limits as $\Gamma \to \infty$, therefore the constant in the δ function in Eq. (A5) can be neglected and the fixed-point distribution will be $f_\Gamma(\zeta) = f_0(\Gamma) e^{-f_0(\Gamma)\zeta}$, where $f_0(\Gamma)$ satisfies the differential equation

$$\frac{df_0(\Gamma)}{d\Gamma} = f_0(\Gamma)[1 - g_0(\Gamma)]. \tag{A6}$$

For $B = 0$, the fixed-point distribution $g_\Gamma(\beta)$ also will be a pure exponential, but, otherwise, it is no longer the case. Assuming that $g_0(\Gamma)$ tends to a finite limit $g_0(\infty)$ as $\Gamma \to \infty$, $f_0(\Gamma)$ will diverge or vanish if $g_0(\infty) < 1$ or $g_0(\infty) > 1$, respectively, as can be seen from Eq. (A6). Thus, at the critical point, we must have $g_0(\infty) = 1$. Here let us assume that $g_0(\Gamma) \simeq 1 + \frac{G}{\Gamma^\gamma}$ and $f_0(\Gamma) \simeq \frac{F}{\Gamma^\phi}$ for large Γ, where G, γ, F, and ϕ are positive constants. Substituting these asymptotic forms into Eq. (A6), we obtain that $\gamma = 1$ and $G = \phi$. Although $g_\Gamma(\beta)$ is not a

pure exponential, its large-β tail is still exponential $g_\Gamma(\beta) \simeq g_1(\Gamma)e^{-g_2(\Gamma)\beta}$, as one can check by substituting it into Eq. (A4). This gives for the unknown functions $g_1(\Gamma)$ and $g_2(\Gamma)$ the differential equations

$$\frac{dg_1(\Gamma)}{d\Gamma} \simeq g_1(\Gamma)[g_0(\Gamma) - f_0(\Gamma) - g_2(\Gamma)], \quad (A7)$$

$$\frac{dg_2(\Gamma)}{d\Gamma} \simeq -f_0(\Gamma)g_1(\Gamma)e^{-Bg_2(\Gamma)}. \quad (A8)$$

Let us assume that these functions have finite limiting values $g_1(\Gamma) \to G_1$ and $g_2(\Gamma) \to G_2$ as $\Gamma \to \infty$. Then, for large Γ, Eq. (A8) assumes the form

$$\frac{dg_2(\Gamma)}{d\Gamma} \simeq -FG_1e^{-BG_2}\Gamma^{-\phi} \equiv -\mathcal{G}\Gamma^{-\phi}. \quad (A9)$$

The finiteness of G_2 then requires $\phi > 1$ and the integration of Eq. (A9) results in

$$g_2(\Gamma) \simeq G_2 + \mathcal{G}\frac{\Gamma^{1-\phi}}{\phi - 1}. \quad (A10)$$

The asymptotic form of Eq. (A7) then reads

$$\frac{dg_1(\Gamma)}{d\Gamma} \simeq G_1\left[1 + \frac{\phi}{\Gamma} - \frac{F}{\Gamma^\phi} - G_2 - \mathcal{G}\frac{\Gamma^{1-\phi}}{\phi - 1}\right]. \quad (A11)$$

For the reason that $g_1(\Gamma)$ converges in the limit $\Gamma \to \infty$, the constant and $O(1/\Gamma)$ terms in the brackets in Eq. (A11) must cancel, which yields $G_2 = 1$, $\phi = 2$, and $\mathcal{G} = 2$. So we conclude that the leading-order Γ dependences of the functions $g_0(\Gamma)$ and $f_0(\Gamma)$ in the critical point are given by

$$g_0(\Gamma) \simeq 1 + \frac{2}{\Gamma}, \quad f_0(\Gamma) \simeq \frac{F}{\Gamma^2}. \quad (A12)$$

The constant F, which takes the value 2 for $B = 0$, remains unknown in the present case.

A relationship between the length scale $\ell(\Gamma) = 1/n(\Gamma)$, where $n(\Gamma)$ is the mean number of nondecimated clusters per unit length of the chain and the rate scale Ω can be derived by solving the differential equation $\frac{dn(\Gamma)}{d\Gamma} = -n(\Gamma)[g_0(\Gamma) + f_0(\Gamma)]$. Using the asymptotic forms

in Eq. (A12), one obtains

$$\ell \simeq \ell_0 e^\Gamma \Gamma^2, \quad (A13)$$

where l_0 is a nonuniversal constant that depends on the initial distribution of parameters.

In order to infer the scaling of the order parameter in the critical point, a further quantity we need is the probability $Q(\Gamma)$ that a given site is part of an active (nondecimated) cluster at the scale Γ. This can be obtained through the probability density $q_\Gamma(\beta)$ of the event that, at the scale Γ, a given site is part of an active cluster that has a logarithmic deactivation rate β. This function evolves according to the equation

$$\frac{\partial q_\Gamma(\beta)}{\partial \Gamma} = \frac{\partial q_\Gamma(\beta)}{\partial \beta} + 2f_0(\Gamma)\left[\int d\beta_1 \int d\beta_2 q_\Gamma(\beta_1)g_\Gamma(\beta_2)\right.$$
$$\left. \times \delta(\beta - \beta_1 - \beta_2 + B) - q_\Gamma(\beta)\right]. \quad (A14)$$

Knowing the large-β tail of $g_\Gamma(\beta)$ only, the best we can do is to determine that of the function $q_\Gamma(\beta)$ from this equation. For large β, the solution will have the form $q_\Gamma(\beta) \simeq [q_1(\Gamma) + q_2(\Gamma)\frac{\beta}{\Gamma}]e^{-g_2(\Gamma)\beta}$, where $q_1(\Gamma)$ and $q_2(\Gamma)$ are unknown functions. Substituting these asymptotic forms into Eq. (A14), we obtain that the above functions must satisfy the differential equations

$$\frac{dq_1(\Gamma)}{d\Gamma} \simeq -\left(1 + \frac{2}{\Gamma}\right)q_1(\Gamma) + \frac{1}{\Gamma}q_2(\Gamma) + O(\Gamma^{-2}q_1(\Gamma)),$$

$$\frac{dq_2(\Gamma)}{d\Gamma} \simeq \frac{\mathcal{G}}{\Gamma}q_1(\Gamma) - \left(1 + \frac{1}{\Gamma}\right)q_2(\Gamma) + O(\Gamma^{-2}q_1(\Gamma)).$$
$$(A15)$$

Since $\mathcal{G} = 2$, these equations are identical to those of the model with $B = 0$. The solutions are $q_1(\Gamma) \simeq c_1e^{-\Gamma}$ and $q_2(\Gamma) \simeq c_2e^{-\Gamma}$, and assuming that the integral $Q(\Gamma) = \int_0^\infty d\beta q_\Gamma(\beta)$ scales with Γ in the same way as the contribution from the large-β tail of $q_\Gamma(\beta)$, we obtain

$$Q(\Gamma) \sim e^{-\Gamma} = \left(\frac{\Omega}{\Omega_0}\right)^{1/\alpha}. \quad (A16)$$

[1] T. E. Harris, Ann. Prob. **2**, 969 (1974).

[2] T. M. Liggett, *Stochastic Interacting Systems: Contact, Voter, and Exclusion Processes* (Springer, Berlin, 2005).

[3] J. Marro and R. Dickman, *Non-Equilibrium Phase Transitions in Lattice Models* (Cambridge University Press, Cambridge 1999).

[4] G. Ódor, *Universality in Nonequilibrium Lattice Systems* (World Scientific, Singapore, 2008); Rev. Mod. Phys. **76**, 663 (2004).

[5] M. Henkel, H. Hinrichsen, and S. Lübeck, *Non-Equilibrium Phase Transitions* (Springer, Berlin, 2008).

[6] D. Mollison, J. R. Stat. Soc. B **39**, 283 (1977).

[7] H. K. Janssen, K. Oerding, F. van Wijland, and H. J. Hilhorst, Eur. Phys. J. B **7**, 137 (1999).

[8] M. E. Fisher, S. K. Ma, and B. G. Nickel, Phys. Rev. Lett. **29**, 917 (1972).

[9] J. Sak, Phys. Rev. B **8**, 281 (1973).

[10] E. Luijten and H. W. J. Blöte, Phys. Rev. Lett. **89**, 025703 (2002).

[11] M. Picco, arXiv:1207.1018; T. Blanchard, M. Picco, and M. A. Rajabpour, Europhys. Lett. **101**, 56003 (2013).

[12] M. C. Angelini, G. Parisi, and F. Ricci-Tersenghi, Phys. Rev. E **89**, 062120 (2014).

[13] H. Hinrichsen and M. Howard, Euro. Phys. J. B **7**, 635 (1999).

[14] F. Ginelli, H. Hinrichsen, R. Livi, D. Mukamel, and A. Torcini, J. Stat. Mech. (2006) P08008.

[15] C. E. Fiore and M. J. de Oliveira, Phys. Rev. E **76**, 041103 (2007).

[16] F. Linder, J. Tran-Gia, S. R. Dahmen, and H. Hinrichsen, J. Phys. A: Math. Theor. **41**, 185005 (2008).

[17] P. Grassberger, J. Stat. Mech. (2013) P04004; J. Stat. Phys. **153**, 289 (2013).

[18] F. Ginelli, H. Hinrichsen, R. Livi, D. Mukamel, and A. Politi, Phys. Rev. E **71**, 026121 (2005).

[19] J. Adamek, M. Keller, A. Senftleben, and H. Hinrichsen, J. Stat. Mech. (2005) P09002.

[20] H. Hinrichsen, J. Stat. Mech. (2007) P07006.
[21] J. Hooyberghs, F. Iglói, and C. Vanderzande, Phys. Rev. Lett. **90**, 100601 (2003); Phys. Rev. E **69**, 066140 (2004).
[22] D. S. Fisher, Phys. Rev. Lett. **69**, 534 (1992); Phys. Rev. B **51**, 6411 (1995).
[23] F. Iglói and C. Monthus, Phys. Rep. **412**, 277 (2005).
[24] R. B. Griffiths, Phys. Rev. Lett. **23**, 17 (1969); B. M. McCoy, *ibid.* **23**, 383 (1969).
[25] A. J. Noest, Phys. Rev. Lett. **57**, 90 (1986); Phys. Rev. B **38**, 2715 (1988).
[26] T. Vojta, J. Phys. A **39**, R143 (2006).
[27] A. M. Reynolds, Phytopathology **101**, 1465 (2011).
[28] R. Juhász, I. A. Kovács, and F. Iglói, Europhys. Lett. **107**, 47008 (2014).
[29] A. B. Harris, J. Phys. C **7**, 1671 (1974).
[30] S. K. Ma, C. Dasgupta, and C.-K. Hu, Phys. Rev. Lett. **43**, 1434 (1979); C. Dasgupta and S. K. Ma, Phys. Rev. B **22**, 1305 (1980).
[31] I. A. Kovács and F. Iglói, Phys. Rev. B **82**, 054437 (2010); **83**, 174207 (2011); J. Phys.: Condens. Matter **23**, 404204 (2011).
[32] R. Juhász, J. Stat. Mech. (2014) P09027.
[33] Y.-C. Lin, H. Rieger, N. Laflorencie, and F. Iglói, Phys. Rev. B **74**, 024427 (2006).
[34] J. Hooyberghs and C. Vanderzande, Phys. Rev. E **63**, 041109 (2001).
[35] We note that this type of rescaling is compatible with the results of the leading ϵ expansion of the nonrandom LRCP; see Ref. [7].
[36] C. J. Neugebauer, S. V. Fallert, and S. N. Taraskin, Phys. Rev. E **74**, 040101(R) (2006); S. V. Fallert and S. N. Taraskin, *ibid.* **79**, 042105 (2009).
[37] T. Vojta and M. Dickison, Phys. Rev. E **72**, 036126 (2005).
[38] J. A. Hoyos, Phys. Rev. E **78**, 032101 (2008).
[39] T. Vojta and J. A. Hoyos, Phys. Rev. Lett. **112**, 075702 (2014); T. Vojta, J. Igo, and J. A. Hoyos, Phys. Rev. E **90**, 012139 (2014).
[40] Disorder-induced crossover effects have been studied in random quantum spin chains; see R. A. Hyman and K. Yang, Phys. Rev. Lett. **78**, 1783 (1997); C. Monthus, O. Golinelli, and Th. Jolicoeur, *ibid.* **79**, 3254 (1997); Phys. Rev. B **58**, 805 (1998); E. Carlon, P. Lajkó, and F. Iglói, Phys. Rev. Lett. **87**, 277201 (2001).
[41] M. A. Muñoz, R. Juhász, C. Castellano, and G. Ódor, Phys. Rev. Lett. **105**, 128701 (2010); R. Juhász, G. Ódor, C. Castellano, and M. A. Muñoz, Phys. Rev. E **85**, 066125 (2012).
[42] R. Juhász and I. A. Kovács, J. Stat. Mech. (2013) P06003.
[43] E. Altman, Y. Kafri, A. Polkovnikov, and G. Refael, Phys. Rev. Lett. **93**, 150402 (2004); Phys. Rev. B **81**, 174528 (2010).